Harmfulness and crack path prediction of branched and radial cracks in disks of shrunk-on disk rotors

C. Stoisser[1], I. Boutemy[2] and **F. Hasnaoui[1]**

[1]EDF R&D, 1 av. de Gaulle, F-92141 Clamart (FRANCE),
carlo.stoisser@edf.fr, frederic.hasnaoui@edf.fr
[2] EDF UTO, av. Montaigne, F-93160 Noisy le Grand (FRANCE), igor.boutemy@edf.fr

ABSTRACT

Inspections revealed stress corrosion cracks in low-pressure shrunk-on disks of nuclear turbines. Cracks initiate in blade attaching pin holes and propagate through the disk in two different ways. First type of crack only propagates in radial direction and second one changes its paths and develops in two different directions (branched crack). This paper deals with the FEM approach used to understand the crack paths propagation and to evaluate the harmfulness of these cracks during over speed start-up. 3D and 2D cracked disk models depending on the size and on the type of cracks have been developed. 2D FE models are validated on 3D FE models by comparing results. Loads due to the rotating blades and to the shrinking effect are taken into account through a contact model introduced at the pin hole surfaces and at the contact surface between the disk and the rotor. The stress intensity factors have been calculated and compared to the fracture toughness. Results show that the crack harmfulness strongly depends on the angular sector of the disk model used in calculations, which is equal to say that the disk lifetime depends on the number of crack affecting the disk. The branched crack path has been explained through the analysis of the G parameter values obtained from the 2D calculations. A good agreement between theoretically predicted and experimental crack path is noticed.

INTRODUCTION

Stress corrosion cracking is a typical failure of nuclear turbine disks operating in wet-to-humid steam transient zone ([1] and [2]). Particularly, ultrasonic inspections in shrunk-on disks have shown cracks in attaching pin holes. Cracking starts at the hole surfaces because of the centrifugal effect due to the blades and develops outwards or inwards in the radial direction. Two or more cracks may joint together in a continuous and transversal crack propagating through the disk in two different ways: first type of crack only propagates in a radial direction; the other one deviates its path from a radial direction and develops in two different directions (branched crack), see [3] and [4]. In this paper, the harmfulness analysis and the crack path prediction concern a Ni-Cr-MO-V disk (Figure 1). For this specific alloy steel, the experimental fracture toughness K_{Ic} is equal to 220 MPa.m$^{1/2}$. Other significant geometric characteristics are:

- Disk radius, R=1.45 m;
- Blade length L=0.19 m
- N° of blades = 302
- Airfoil mass, m_v=1.15 Kg
- Pin diameter, d=0.007 m

Rotating speed ω changes from 1500 rpm (nominal conditions) to 2250 rpm (accidental conditions). Shrinkage is nil at ω=1800 rpm because of centrifugal forces.

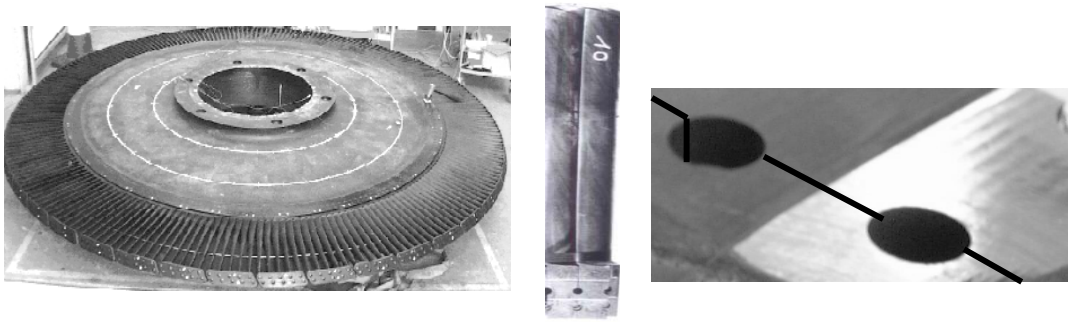

Figure 1: Shrunk-on bladed disk (left), blades with attaching pin (centre), a zoom on the disk pin holes (right)

First objective of the work is to analyse the harmfulness of only one crack affecting the disk, i.e. the critical depth that determines the brittle fracture, related to the different operating speeds. Second objective is to provide an explanation for the bifurcation angle of the branched cracks observed in structural components. Given results are based on the potential energy release rate, G, and on the stress intensity factors, SIF, obtained from 2D and 3D calculations. Plasticity effects are not taken into account in this study.

THE FINITE ELEMENT MODEL

Cracked disk 3D and 2D FE models are realised taking into account the centrifugal forces and the shrinkage effect. 2D models are adjusted on the 3D model results (which are high time consumers) in order to carry out a great number of simulations.

The meshing consists of an angular sector of the rotor, the cracked disk and the blades, where α° is its angular amplitude. Symmetry conditions are imposed to the right and to the left faces of the model. The whole disk is consequently consider as a set of *n* sectors, which are equivalent to the studied model ($n=360°/\alpha°$). The whole disk will have a number *m* of defects, which depends on the angular amplutide of the sector and on the crack position. For istance, if α=90° and the crack is in the middle of the sector, the model allows studying the harmfulness of a disc with 4 cracks. If α=90° and only one face of the crack is modelled and located on one of the two sector sides, the effect of only 2 crack is simulated. This approach is possible when α is an integer factor of *360°*. Once the number of modelled blades is fixed, α is automatically given: α is never

an integer factor of 360°, except for 302 blades, i.e. α=360°, and for 151 blades, i.e. α=180°. In this latter case, disk will have 2 defects, if crack is located in the centre of the sector, or only 1 defect, if one of the crack faces is located on one of the two sector sides. In order to predict the harmfulness related to only one crack, 3D calculations on a 180° sector are too heavy to be performed: the use and the validation of the 2D model is necessary.

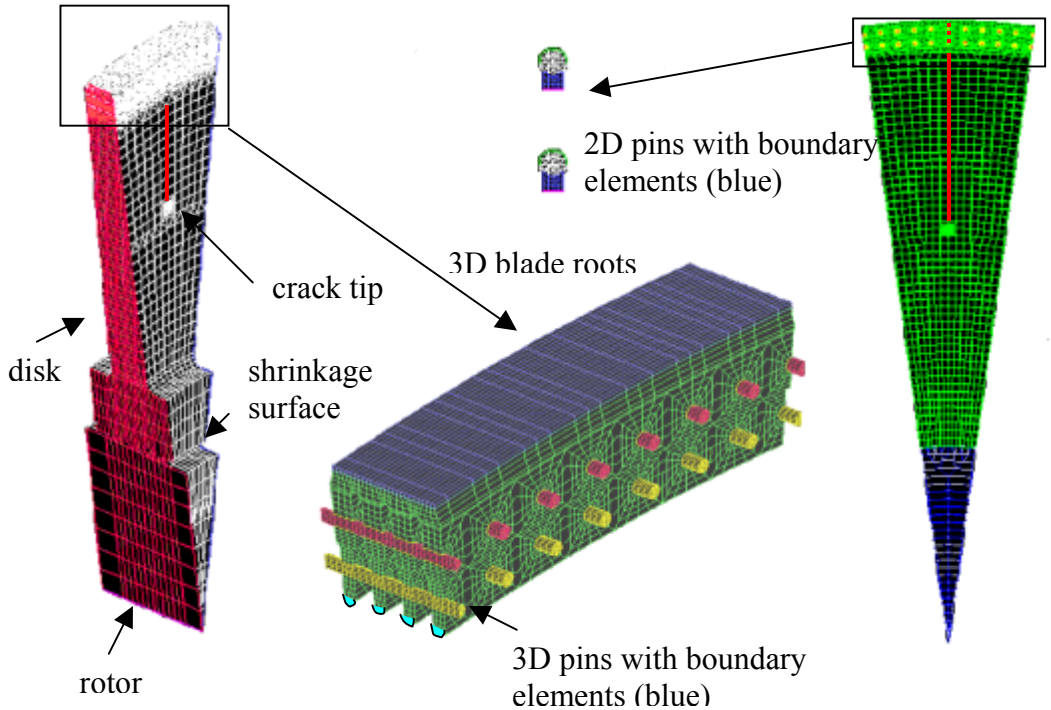

Figure 2: 3D FE and 2D models, angular amplitude α=11.92°

Centrifugal and shrinkage loads

Disk and rotor centrifugal forces obviously depends on the given rotating speed, $\vec{F} = \rho\,\omega^2 r\,\vec{u}_r$, where ρ is the 3D and 2D density (ρ_{3D} and ρ_{2D}) of FE representing disk and rotor. In 3D models, pins and blade roots are also completely modelled. The centrifugal force due to the airfoil is taken into account by means of a FE thickness, the density of which (ρ_{eq3D}) is adjusted. In 2D models, the blade centrifugal load is directly distributed on the two corresponding pins: the material density of the finite elements representing pins (ρ_{eq2D}) takes into consideration pin and blade actions. Unilateral contact conditions between the pins and the pin holes are used for a more realistic load representation.

When ω=0 rpm, the rotor external surface meshing penetrates the internal disk surface meshing in radial direction according to the shrinkage value. Centrifugal forces and a contact algorithm allow for the correct modelling of the shrinkage effects.

Boundary conditions

Rigid body displacements of model parts working under contact conditions (disk, root blades and pins in 3D models and disk and pins in 2D model) must to be blocked.

Symmetry conditions allow the right boundary conditions in the transversal plan for the disk while highly deforming finite elements are introduced to clamp pins in radial direction. At last, 3D rotor and disk displacements in axial direction are imposed equal to zero without stress adding in structure.

Crack tip modelling

Quadratic meshing with Barsoum's type elements [5] is used for 2D and 3D crack tip models: in order to perform more accurate SIF calculations, the central node of the mesh edge is moved to a position corresponding to a quarter of the edge length.

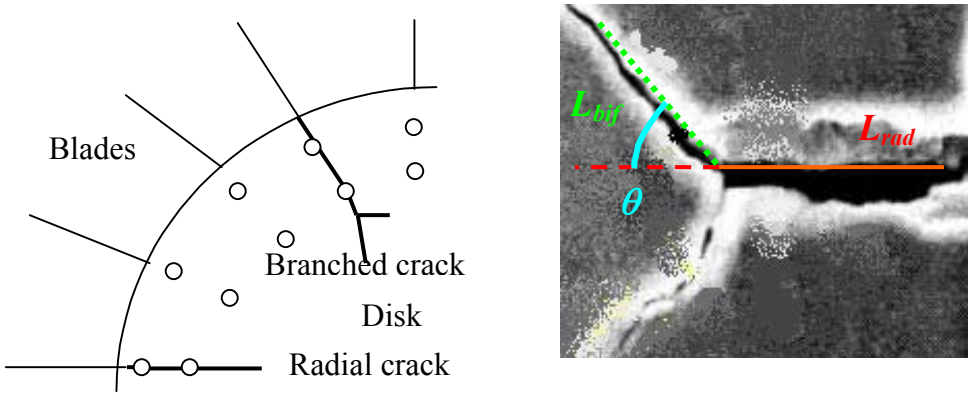

Figure 3: Simplified disk view with radial and branched cracks (left), bifurcated crack geometry and parameters nomenclature (right, adapted from [4])

HARMFULNESS OF RADIAL CRACKS

First calculations concern transversal cracks "cutting" disk in two parts at holes and having a variable depth *x* measured from the disk external surface. The SIF are obtained using the energetic method: once G is calculated, the Irwin's formula, [6], is used and the SIF obtained from 2D calculations are determined under the hypothesis of plane strains or stresses.Since centrifugal loads induce a dominant I mode growth direction with respect to II and III modes, to calculate SIF from 3D results, following hypothesis are given: 1) the problem is symmetric and 2) 2D plane strain solutions and 2D plane stress solutions are the upper and lower limits of the 3D case.

Therefore, the 2D Irwin's formula gives for the 3D problem: $\sqrt{GE} \le K_I \le \sqrt{\frac{GE}{1-\nu^2}}$, where G is the maximal value of the potential energy relate rate calculated at the crack tip, *E* the Young's modulus and ν the Poisson's number. The harmfulness analysis is performed comparing K_I, which is calculated according to its upper limit, to K_{Ic}.

Simulations and post-processing are carried out by means of *Code_Aster*©, [7]. Following results are obtained by modelling only one face of the crack on one of the sector sides. Table 1 shows K_I calculated at the tip of a transversal crack, the depth of which is equal to 20% of the disk diameter, for simulations at ω=2250 rpm. K_I are obtained from 3D and 2D calculations both. Table 1 also shows τ, which is the ratio of K_{I_α}, obtained for the given sector, on $K_{I\_11.92°}$, obtained for a FE sector, the amplitude of which is α=11.92°. As expected, the angular amplitudes of 2D and 3D models both have a big influence on the numerical results. However, the evolution of K_I as a function of α is very similar in 2D and 3D models. 2D calculations provide a good prediction of the 3D effects due to the increase of α. Differences between 2D and 3D results are due to the non-uniform thickness of the 3D model (see [8]).

Table 1: 3D and 2D results, ω=2250 rpm, x=288 mm

α	3D		2D – plane stresses		2D – plane strains	
	K_I	τ	K_I	τ	K_I	τ
11.92°	184.5	1	239.0	1	230.6	1
21.92°	243.4	1.32	314.2	1.31	301.4	1.31
46.92	318.2	1.73	412.9	1.73	394.1	1.71
90° (2 cracks)	362.3	1.96	473.5	1.98	451.2	1.96

2D FE models are consequently adjusted to the 3D results: 2D FE material density is adjusted in proportion to the ratio $K_{I\_3D\_\alpha}/K_{I\_2D\_\alpha}$, where $K_{I\_3D\_\alpha}$ is the K_I obtained from 3D calculations and $K_{I\_2D\_\alpha}$ the K_I obtained from 2D calculations. Concerning previous case, since FE material densities are $\rho_{2D}= \rho_{3D}$=7800 kg/m^3 and $\rho_{eq2D}= \rho_{eq3D}$=30206 kg/m^3, new 2D FE densities are ρ_{2D}=6021 kg/m^3 and ρ_{eq2D}=23317 kg/m^3 (plane stresses modelling) and ρ_{2D}=6241 kg/m^3 and ρ_{eq2D}=24169 kg/m^3 (plane strains modelling). New results are shown in Table 2: 2D and 3D K_I are very similar. A 2D 180° FE model can then be used to predict the one crack harmfulness (see last row on Table 2).

Table 2: 3D and 2D results, ω=2250 rpm, x=288 mm, after adjusting

α	3D		2D – plane stresses		2D – plane strains	
	K_I	τ	K_I	τ	K_I	τ
11.92°	184.5	1	184.5	1	184.5	1
21.92°	243.4	1.32	242.5	1.31	241.1	1.31
46.92	318.2	1.73	318.6	1.73	315.3	1.71
90° (2 cracks)	362.3	1.96	365.4	1.98	360.9	1.96
180° (1 crack)			367.2	1.99	362.8	1.97

There is not an important difference between plane stresses and plane strain results. It is observed the results obtained from 90° and 180° models are close: since only one crack face is modelled on one sector side, we can conclude that the one crack harmfulness is very close to the harmfulness of two cracks located in opposite side with respect to the disk centre. When crack depth is given, the 2D adjusting to 3D results depends on the considered rotating speed: the shrinkage effect on the crack tip changes according to ω. When rotating speed is given, is also noticed the adjusting depends on the crack depth because the disk thickness rises getting closer to the axis. 2D models are not able to take into consideration variations in the disk geometry and in the crack tip length. Figure 4 illustrates a summary of results: for one crack the critical radial depth before brittle fracture is equal to about 10% of the disk diameter length at the maximum overspeed (2250 rpm).

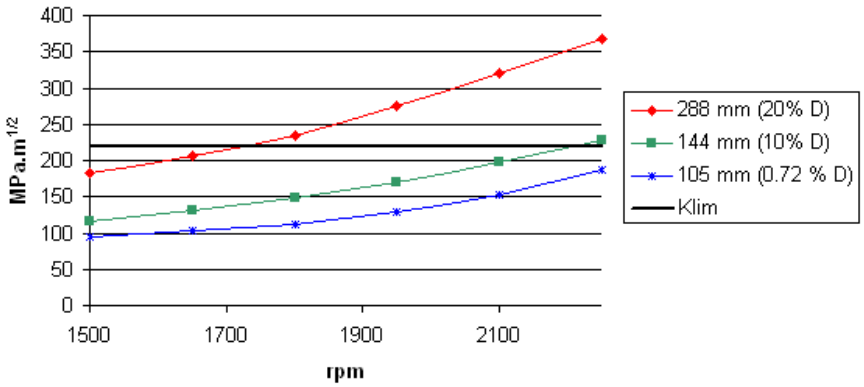

Figure 4: One radial crack harmfulness' prediction

BRANCHED CRACK PATH PREDICTION

Two criteria are generally used for the prediction of the crack growth direction, [9]: 1) the direction in which G is maximum and 2) the direction which annuls K_{II} (if K_{III}=0).

Calculations are performed on 2D models (under hypothesis of plane strains). A half crack, the face of which is located on one of the sector sides, is modelled. Following parameters are taken into account, according to the picture of Figure 3 (right):

- L_{rad}=78.5mm
- L_{bif}=10mm
- $3.57° \leq \alpha \leq 180°$
- $0° \leq \theta \leq 30°$

In order to apply criterion 1., the potential energy release rate, which is calculated on one branch, has to be compared to the half value of G related to the radial crack.

Figure 5 shows that branched cracks can propagate with a bifurcation angle θ = 21°. It is also noticed that G calculated for a branched crack ups 8% on G calculated for a radial crack (θ=0°). From graphs of Figure 6, we can deduce that criterion based on K_{II} gives a bifurcation angle θ=23°; θ is constant and equal to 25° from α>28°. Figure 6-right, the ratio of G_{rad} (the potential energy release rate calculated with θ=0°) and G_{bif} calculated with θ that maximizes G) is constant and equal to 10.8%° from α>28°.

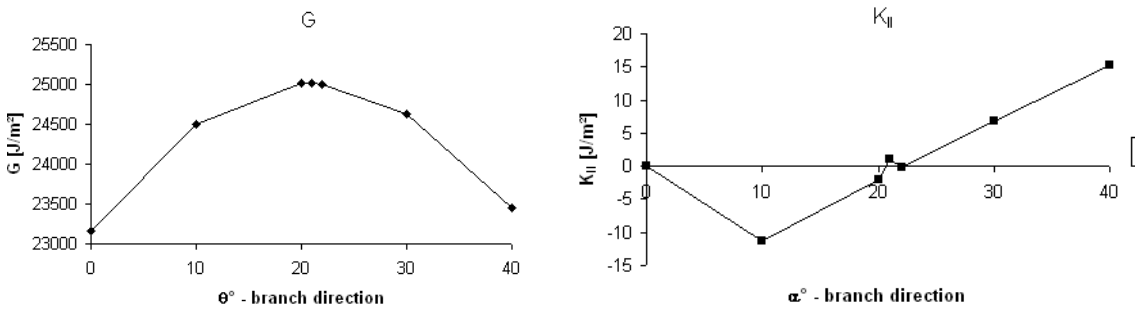

Figure 5: G and K_{II} as a function of the angle θ between radial and branch directions

Branched cracks can appear with a bifurcation angle 2θ=55°. Results are in good accordance with experimental values (branched cracks have been found with 55°<2θ<60°).

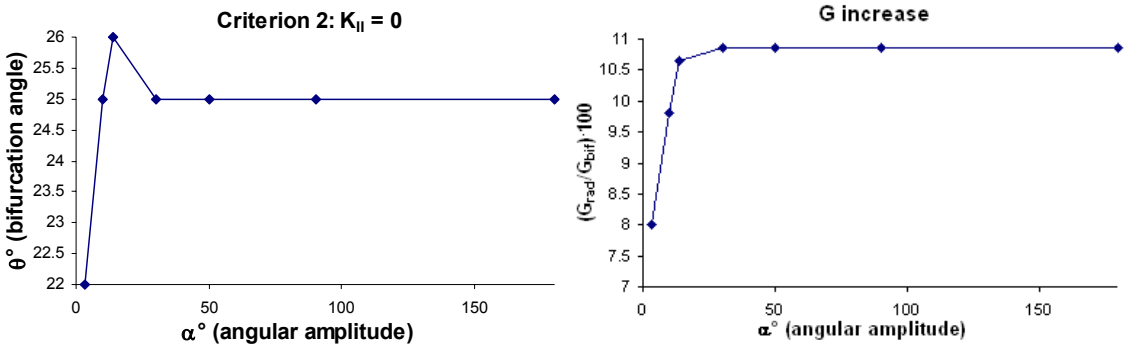

Figure 6: Harmfulness of cracks as a function of the angle of the modelled disk sector

Finally, Table 3 and Table 4 show influence of the branch length L_{bif} and the bifurcation depth L_{rad} on the results. The rate observed with L_{bif}=10mm is well confirmed even if θ weakly increases for smaller lengths of L_{bif}. The bifurcation depth does not have influence on θ, except when the bifurcation point is very close to the pin hole and boundary effects are note negligible.

Table 3: Influence of the branch length L_{bif}

	L_{bif}=10mm	L_{bif}=5mm	L_{bif}=2.5mm
Bifurcation angle θ (criterion 2)	22°	23°	24°
Increase of G (criterion 1)	8%	8.6%	9.2%

Table 4: Influence of the bifurcation depth L_{rad}

	L_{rad}=58.5mm	L_{rad}=68.5mm	L_{rad}=78.5mm	L_{rad}=88.5mm
Bifurcation angle θ (criterion 2)	24°	22°	22°	22°
Increase of G (criterion 1)	8.3%	8%	8%	8%

CONCLUSION

The harmfulness and the crack path prediction of branched and radial cracks in bladed disk have been presented in this paper. For one defect, numerical results based on 2D and 3D calculations show that the critical radial depth before brittle fracture is equal to 10% of the disk diameter length at the maximum overspeed (2250 rpm). This conclusion is still valid when two cracks are located in the disk in opposite side with respect to the disk centre. Concerning the branched crack path prediction, the criterion based on K_{II}=0 seems to be adapted to describe the real phenomena because radial crack and bifurcated cracks both are identified. Numerical bifurcation angles are close to the experimental ones.

REFERENCES

1. Lyle F.F., Mc Minn A. and Leverant G.R. (1985), *Proc Instn Mech Engrs* **Vol 199** A1.
2. Lyle F.F. and Burghard H.C. (1982). In: *Steam turbine disk cracking experience*, EPRI NP-2429-LD, Vol. 1-7
3. Shi H.J., Niu L.S., Mesmacque G. and Wang Z.G. (2002), *Int. J. Fatigue* **Vol 22**, 457 - 465
4. Meggiolaro M.A., Miranda A.C.O., Castro J.T.P and Martha L.F. (2003). In: *2nd MIT Conference on Computational Fluid and Solid Mechanics,* 432 – 435
5. Lemaître J., Chaboche J.L. (1996). In: *Mécanique des matériaux solides*, Dunod
6. Bui H.D. (1978). In: *Mécanique de la rupture fragile*, Masson
7. Code_Aster, (2004). *Numerical simulation software for structural analysis,* http://www.code-aster.org
8. Stoisser C.M. (2004). *Harmfulness analysis of pin hole disk cracking*. EDF R&D Internal Report N°HT-65/04/018
9. Amestoy M., Bui H.D. and Dang Vang (2002). In: *Academie des Sciences Paris, Internal Report*, t.289, series B99.